Dye-Sensitized Solar Cells

DOI: 10.1002/anie.201300070

Stable Dye-Sensitized Solar Cell Electrolytes Based on Cobalt(II)/(III) Complexes of a Hexadentate Pyridyl Ligand**

Muhammad K. Kashif, Michael Nippe, Noel. W. Duffy, Craig M. Forsyth, Christopher J. Chang, Jeffrey R. Long,* Leone Spiccia,* and Udo Bach**

Dye-sensitized solar cells (DSCs) can be fabricated from low-cost components with simple high-throughput printing techniques thereby providing a viable alternative to conventional photovoltaics.[1] A recent step-change in DSC research has been the successful application of transition-metal complexes (e.g., $[Co(bpy)_3]^{2+/3+}$, bpy = 2,2′-bipyridine), organometallics (e.g., ferrocene), and organic compounds as redox mediators,[2,3] replacing formerly used corrosive iodine/iodide electrolytes while maintaining impressive energy conversion efficiencies.[4]

An attractive feature of cobalt complexes, in particular, is that the structure, electronic properties, and redox chemistry can be tuned by varying the ligand environment. In this respect, the type and number of donor atoms (denticity) that the ligands used to form the cobalt coordination sphere is of paramount importance. First, for related families of ligands, such as polypyridyls, a higher denticity results in a higher overall stability constant (β) of the complex through the chelate effect.[5] The stability of complexes is important when contemplating their application in many fields, including renewable energy research focusing on DSCs and solar-driven hydrogen generation from water. Dissociation of the bpy ligands from $[Co(bpy)_3]^{2+}$ was recently identified as a significant issue for its applicability as a catalyst in photo-electrochemical water splitting devices, which was overcome by replacing the bpy ligands with a pentadentate ligand.[6] Secondly, the denticity of the ligands will affect the reorganization energies associated with electron transfer processes involving the $Co^{2+/3+}$ redox states,[7] and will influence the rates of important charge-transfer steps, such as charge recombination and dye regeneration. The latter will affect the driving force required for efficient dye regeneration and therefore ultimately the maximum obtainable DSC efficiency.[8,9]

To date only a small number of cobalt complexes have been tested in DSCs, with the majority based on bidentate ligands such as bpy and phen (1,10-phenanthroline) and their derivatives. In a recent article about applying $Co^{II/III}$-tpy complexes (tpy = 2,2′;6′,2″-terpyridine) as DSC redox mediators, Grätzel and co-workers highlight the importance of ligand substitution to achieve higher open-circuit photovoltage (V_{OC}).[3g] We recently reported a study of DSCs employing cobalt complexes based on a combination of a pentadentate ligand (2,6-bis(1,1-bis(2-pyridyl)ethyl)pyridine, $PY5Me_2$) and a weakly bound monodentate ligand. We were able to fine-tune the redox potential of the complex by choosing monodentate ligands with varying Lewis basicity, thereby creating the opportunity to adjust the driving force for dye regeneration.[10] Here we report for the first time the application of the Co complex of a hexapyridyl ligand (6,6′-bis(1,1-di(pyridin-2-yl)ethyl)-2,2′-bipyridine, bpyPY4) as a redox mediator in DSCs, and compare its photovoltaic performance and stability to the reference mediator $[Co(bpy)_3]^{2+/3+}$ (Co-bpy). A major motivation for using a hexadentate ligand was to develop a redox shuttle based on complexes with very high thermodynamic stability.

[*] M. K. Kashif, Prof. Dr. U. Bach
Department of Materials Engineering, Monash University
Clayton, Victoria 3800 (Australia)
E-mail: udo.bach@monash.edu

Dr. M. Nippe, Prof. Dr. J. R. Long
Department of Chemistry, University of California
Berkeley, CA 94720-1460 (USA)
E-mail: jrlong@berkeley.edu

Prof. Dr. C. J. Chang
Departments of Chemistry and Molecular and Cell Biology
and the Howard Hughes Medical Institute
University of California, Berkeley, CA 94720-1460 (USA)
E-mail: chrischang@berkeley.edu

Dr. M. Nippe, Prof. Dr. C. J. Chang, Prof. Dr. J. R. Long
Materials or Chemical Sciences Division
Lawrence Berkeley National Laboratory
Berkeley, CA 94720-1460 (USA)

Dr. C. M. Forsyth, Prof. Dr. L. Spiccia
Department of Chemistry, Monash University
Clayton, Victoria 3800 (Australia)
E-mail: leone.spiccia@monash.edu

Prof. Dr. U. Bach
Melbourne Centre for Nanofabrication
151 Wellington Road, Clayton, Victoria 3168 (Australia)
and
CSIRO, Materials Science and Engineering
Clayton South, Victoria 3169 (Australia)

N. W. Duffy
CSIRO, Energy Technology
Clayton South, Victoria 3169 (Australia)

[**] The authors acknowledge the Australian Research Council for providing equipment and fellowship support and the Australian Solar Institute, the Victorian State Government (DBI-VSA and DPI-ETIS) for financial support. The CSIRO is acknowledged for providing support through an OCE Science Leader position (UB). Part of the synthetic work was carried out at the Joint Center for Artificial Photosynthesis supported by the Office of Science of the U.S. Department of Energy under award number DE-SC0004993.

Supporting information for this article, including details of the synthesis, device characterization, and crystal structure determination, is available on the WWW under http://dx.doi.org/10.1002/anie.201300070.

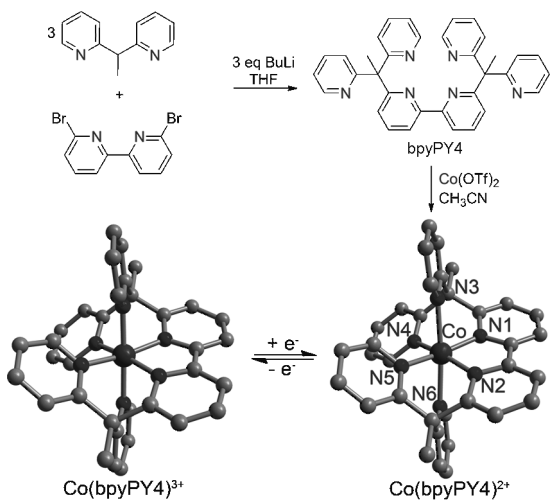

Figure 1. Synthetic route to bpyPY4 and molecular structures of $[Co(bpyPY4)]^{2+/3+}$ in crystals of **1a**/**1b**.

Full details of the synthesis and characterization of bpyPY4, $[Co(bpyPY4)](CF_3SO_3)_2$ (**1a**) and $[Co(bpyPY4)](CF_3SO_3)_3$ (**1b**) (CF_3SO_3 = trifluoromethanesulfonate) are in the Supporting Information. In brief, the new bpyPY4 ligand was synthesized through the reaction of deprotonated 1,1-bis(2-pyridyl)ethane and 6,6′-dibromo-2,2′-dipyridyl (Figure 1). Complexation of bpyPY4 with $Co(CF_3SO_3)_2$ in acetonitrile (MeCN) and subsequent crystallization from MeCN/Et_2O yielded dark red crystals of **1a**. Oxidation of **1a** with stoichiometric amounts of $Ag(CF_3SO_3)$ afforded **1b**, which could be crystallized by Et_2O diffusion into a MeCN solution. The results of the crystal structure analyses are depicted in Figures 1, S1, S2, and Table 1. Comparison of the

Table 1: Metal ligand bond lengths in **1a** and **1b**.

Compound	**1a** [Å]	**1b** [Å]
Co–N1	1.926(2)	1.929(3)
Co–N2	1.941(4)	1.917(3)
Co–N3	2.216(3)	1.952(3)
Co–N4	1.965(4)	1.944(3)
Co–N5	1.955(4)	1.940(3)
Co–N6	2.235(3)	1.943(3)

Co–N bond lengths for cobaltous **1a** and cobaltic **1b** reveals that the major change upon oxidation of the Co^{II} to the Co^{III} complex is a contraction along the N3–Co–N6 axis, with relatively minor changes to the equatorial bond lengths (Table 1). In contrast, all Co–N bond lengths in $[Co(bpy)_3]^{2+/3+}$ and $[Co(PY5Me_2)NMBI]^{2+/3+}$ changed significantly.[10,11] The rigidity of the preorganized cavity of the hexadentate ligand appears to restrict structural changes upon reduction/oxidation to axial elongation/compression of the cobalt(II)/(III) coordination sphere (NMBI = *N*-methylbenzimidazole).

The cyclic voltammogram of **1a** in MeCN (0.1 M NBu_4PF_6; Figure S3) shows reversible processes centered at −170 and −90 mV vs. Fc/Fc^+ corresponding to the $[Co(bpyPY4)]^{2+/3+}$ and $[Co(bpyPY4)]^{1+/2+}$ redox reactions, respectively (Fc = ferrocene). Features observed at more negative potentials are ascribed to ligand-based reduction processes. Thus, the redox potential related to $Co^{2+/3+}$ in **1a** is calculated to be 465 mV versus the normal hydrogen electrode (NHE), whereas the corresponding redox potential for $[Co(bpy)_3]^{2+/3+}$ is 560 mV. The cathodic and anodic current responses associated with the Co-based redox processes are linearly proportional to the square root of the scan rate (ν), indicating diffusion-controlled behavior as is expected for a homogeneous system. A comparison of the redox potentials (vs. NHE) for **1a**/**1b**, $[Co(bpy)_3]^{2+/3+}$, and the $E(D/D^+)$ levels of MK2 (Figure 2) reveals that **1a**/**1b** will provide a substantial

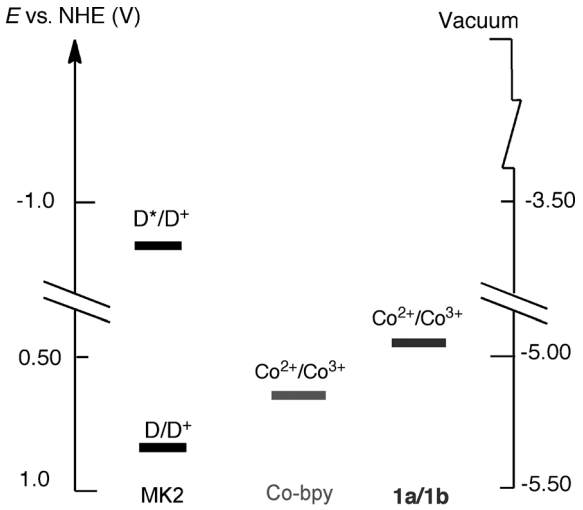

Figure 2. Energy level diagram showing the approximate redox potentials of DSC components relative to the normal hydrogen electrode (NHE) in acetonitrile.

electrochemical driving force for dye regeneration (> 400 mV). The redox properties of **1a** indicate that it is well suited for DSC electrolyte development using dyes with $E(D/D^+)$ energies ≥ 800 mV vs. NHE. In this study, MK2, a dye with a high molar extinction coefficient of $38\,400\ M^{-1}cm^{-1}$ and excellent light-harvesting properties was considered a good photosensitizer for use with one-electron-transfer redox couples.[12]

The **1a**/**1b**-based electrolytes were optimized by varying the concentrations of **1a**, **1b** and the additives, NMBI and lithium bis(trifluoromethanesulfonyl)imide (LiTFSI). The data for the optimized devices are shown in Table 2. Previously, we have shown that very thin (1 μm) transparent titania films can be successfully used to harvest most of the incident light.[10] However, in this study, we have successfully applied thicker titania films, consisting of 6 μm transparent layers of 30 nm particles coated with 4 μm thick scattering layers (400 nm particles). With these 10 μm mesostructured films, an efficiency of 7.8% for the MK2/Co-bpy electrolyte combination was achieved, which is higher than reported recently (7.3%).[12a] An impressive efficiency of 8.3% was achieved for the DSCs based on the new redox couple **1a**/**1b**. A reduction in V_{OC} of 100 mV is observed for **1a**/**1b**-based

Table 2: Photovoltaic performance of DSCs assembled with the two redox couples and MK2 dye with simulated sunlight (AM 1.5 G, 1000 $W m^{-2}$).[a]

Redox couple[b]	**1a**/**1b**	Co-bpy
$E_{1/2}(Co^{2+/3+})$ [mV][c]	465	560
V_{OC} [mV]	757 ± 2	826 ± 3
J_{SC} [mA cm^{-2}]	14.7 ± 0.2	13.7 ± 0.3
FF	0.75 ± 0.02	0.69 ± 0.01
η [%]	8.3 ± 0.1	7.8 ± 0.2

[a] Double-layer TiO_2 films [6 μm mesoporous TiO_2 (30 nm) and 4 μm scattering TiO_2 (400 nm)] and a Pt counter electrode were used for the fabrication of all DSCs. The devices were measured immediately after fabrication and the average performance of at least three devices with standard deviation is provided. [b] The electrolyte consists of 0.20 M Co^{II} complex, 0.10 M of Co^{III} complex, 0.05 M of LiTFSI and 0.50 M of NMBI in pure acetonitrile (MeCN). [c] Redox potentials of the **1a** and Co-bpy are reported vs NHE.

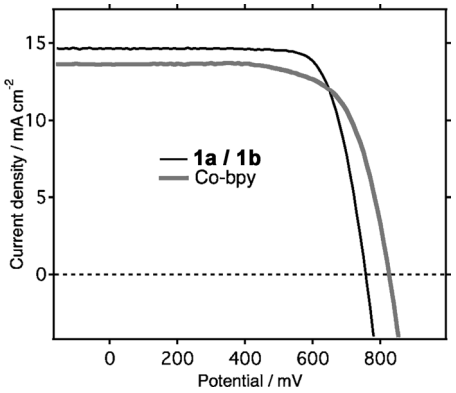

Figure 3. Current density (*J*)–potential (*V*) characteristics of the best-performing DSCs fabricated using electrolytes **1a**/**1b** and Co-bpy. For photovoltaic performance data and details on the electrolyte composition see Table 2.

devices, as compared to Co-bpy-based devices, which is in agreement with the about 100 mV difference in the $Co^{II/III}$ redox potentials of **1a** and Co-bpy.

Figure 3 shows the current density (*J*)–potential (*V*) characteristics of the best performing DSCs based on redox couples **1a**/**1b** and Co-bpy, measured under simulated air mass (AM) and 1.5 G, 1000 $W m^{-2}$. The electrolyte included NMBI as an additive. The devices employing **1a**/**1b** in the electrolyte show a higher current density (J_{SC}) and a significant increase in the fill factor (*FF*) compared to the devices based on Co-bpy, indicating that **1a**/**1b** clearly outperforms Co-bpy as a redox mediator. This is likely due to the lower electrochemical driving force for dye regeneration in case of Co-bpy ($\Delta E = 340$ mV), compared to **1a**/**1b** ($\Delta E = 435$ mV). This is in agreement with previous studies on DSCs employing cobalt mediators, where the minimum electrochemical driving force for quantitative dye regeneration was found to be around 500 mV.[3b,h] Furthermore, light soaking the devices made with **1a**/**1b** for 20 min under AM 1.5 G and 1000 $W m^{-2}$ irradiation resulted in an increase in J_{SC} and a slight decrease in V_{OC}, giving rise to an overall efficiency of 9.4% (see Table S2). Similar light-soaking effects have been previously linked to a shift in conduction band edge.[13] The incident photon-to-electron conversion efficiency (IPCE) spectra of DSCs, made using either electrolytes are comparable (see Figure S5) with a few percent higher IPCE for **1a**/**1b** resulting in a slight increase in J_{SC}.

Intensity-modulated photovoltage spectroscopy (IMVS), complemented by charge extraction measurements, was used to compare the electron lifetimes for DSCs assembled with **1a**/**1b** and Co-bpy-based electrolytes as a function of the extracted charge (Figure 4). Interestingly, the two DSCs

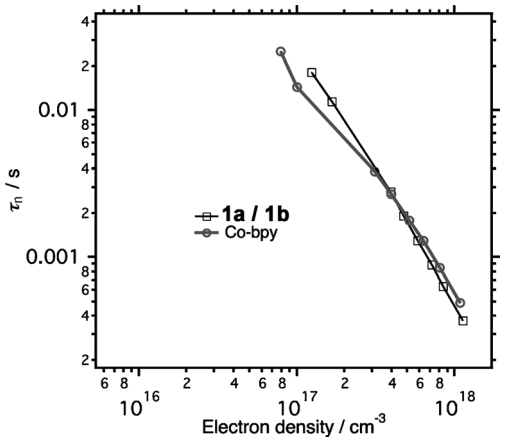

Figure 4. Electron lifetime (τ_n) determined via IMVS spectroscopy versus extracted charge for DSCs based on electrolyte **1a**/**1b** and Co-bpy. The electron density per volume of mesoporous TiO_2 film was determined by charge extraction experiments.

exhibit similar lifetimes for the electrons injected into the TiO_2 conduction band, indicating comparable charge-recombination rates for both electrolyte systems.

The evolution of DSC performance for devices based on **1a**/**1b** and Co-bpy redox mediators was also tested under continuous simulated full sun irradiation. In this comparison, we also studied the effect of additives on device stability by using two different Lewis base additives. Keeping in mind that the Lewis bases added to the electrolytes may interact with the polypyridyl complexes, a comparatively milder Lewis base, *p*-trifluoromethylpyridine (TFMP), was examined as an electrolyte additive in parallel to NMBI, which is commonly applied in iodide/triiodide-based DSCs to improve the long-term stability.[14] In choosing TFMP, the excellent thermal, hydrolytic, and oxidative stability of fluorinated aromatic hydrocarbons and the relatively small size of the $-CF_3$ group were considered beneficial features.[15] The *J*–*V* results for cells fabricated using **1a**/**1b** and Co-bpy using TFMP as an additive are shown in Table S1 and Figure S5. The addition of TFMP to Co-bpy leads to a green precipitate and, as a consequence, the devices made with this electrolyte show poor performance reproducibility and very poor stability. In contrast, no precipitation was observed in the **1a**/**1b**/TFMP electrolytes and the DSCs gave comparable efficiencies to the **1a**/**1b**/NMBI electrolyte system.

Preliminary stability tests were then carried out to compare devices with NMBI and TFMP added to **1a**/**1b**

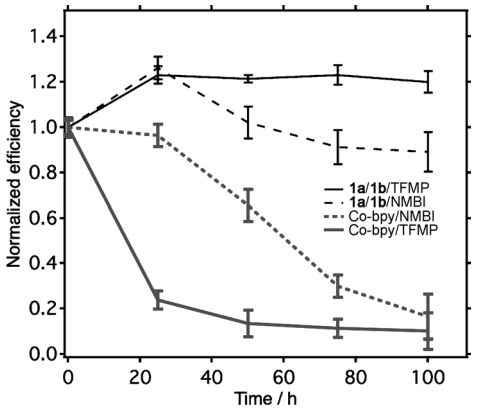

Figure 5. Normalized efficiencies of the devices under full sun irradiation aging experiment is shown with a 400 nm UV-cut off filter. Two Lewis bases, NMBI and TFMP, were alternatively used with **1a**/**1b** and Co-bpy (4:1, MeCN:VN).

and Co-bpy-based electrolytes abbreviated **1a**/**1b**/NMBI, **1a**/**1b**/TFMP, Co-bpy/NMBI, and Co-bpy/TFMP (Figure 5).

A mixture of acetonitrile and valeronitrile (4:1) was used to reduce the volatility of the electrolyte. An environmental chamber equipped with a Hg lamp was automated to maintain the DSCs under continuous full sun irradiation at 45% humidity and a device temperature of 25–30°C to test the devices. Figure 5 shows the normalized efficiencies of the DSCs over a period of 100 h. DSCs based on electrolyte **1a**/**1b** clearly outperformed those assembled with the reference mediator Co-bpy, showing a >20% performance increase over the first 24 h of continuous illumination. When TFMP was used, the DSCs based on **1a**/**1b** initially showed a 20% increase in performance, which maintained across the full 100 h testing period. In the case of NMBI, the DSCs showed the same initial improvement in performance but there was a gradual decrease and stabilization at about 90% of the original value after 100 h testing. Over the 100 h period, a decrease in performance of over 80% was observed for DSCs based on the Co-bpy electrolyte and NMBI. In the presence of TFMP, this performance decrease was even more pronounced, with a drop of 76% observed after the first 24 h illumination period. In general, the Co-bpy electrolyte was found to be incompatible with TFMP, leading to a green precipitate and poor device performance.

In conclusion, we have prepared and structurally characterized the Co^{II} and Co^{III} complexes of a new hexadentate polypyridyl ligand and, for the first time, applied such types of complexes as redox mediators in DSC electrolytes. The devices constructed with these complexes were found to outperform the prototypical Co-bpy redox mediator both in terms of overall efficiency and stability under full sun irradiation conditions. The design of multidentate ligands leading to very stable cobalt complexes under DSC test conditions is likely to become a major area of endeavor in the quest for high-performance cobalt-based DSC electrolytes that meet the stringent stability requirements of commercial applications. For further optimization of the cobalt-based redox mediators, studies are underway to evaluate the minimum electrochemical energy required for quantitative dye regeneration in line with our previous work on ferrocene derivatives.[16]

Received: January 4, 2013
Revised: March 19, 2013
Published online: April 18, 2013

Keywords: cobalt electrolytes · dye-sensitized solar cells · energy conversion · ligand engineering

[1] a) M. Graetzel, R. A. J. Jenssen, D. B. Mitzi, E. H. Sargent, *Nature* **2012**, *488*, 304–312; b) F. Kato, A. Kikuchi, T. Okuyama, K. Oyaizu, H. Nishide, *Angew. Chem.* **2012**, *124*, 10324–10327; *Angew. Chem. Int. Ed.* **2012**, *51*, 10177–10180.

[2] a) S. Powar, T. Daeneke, M. T. Ma, D. Fu, N. W. Duffy, G. Gotz, M. Weidelener, A. Mishra, P. Baeuerle, L. Spiccia, U. Bach, *Angew. Chem.* **2013**, *125*, 630–633; *Angew. Chem. Int. Ed.* **2013**, *52*, 602–605; b) T. Daeneke, Y. Uemura, N. W. Duffy, A. J. Mozer, N. Koumura, U. Bach, L. Spiccia, *Adv. Mater.* **2012**, *24*, 1222–1225; c) T. Daeneke, T. H. Kwon, A. B. Holmes, N. W. Duffy, U. Bach, L. Spiccia, *Nat. Chem.* **2011**, *3*, 211–215; d) J. Liu, J. Zhang, M. Xu, D. Zhou, X. Jing, P. Wang, *Energy Environ. Sci.* **2011**, *4*, 3021–3029; e) H. Tian, Z. Yu, A. Hagfeldt, L. Kloo, L. Sun, *J. Am. Chem. Soc.* **2011**, *133*, 9413–9422; f) J.-H. Yum, E. Baranoff, F. Kessler, T. Moehl, S. Ahmad, T. Bessho, A. Marchioro, E. Ghadiri, J.-E. Moser, C. Yi, M. K. Nazeeruddin, M. Grätzel, *Nat. Commun.* **2012**, *3*, 631–638; g) M. Wang, N. Chamberland, L. Breau, J.-E. Moser, R. Humphry-Baker, S. M. Zakeeruddin, M. Grätzel, *Nature Chem.* **2010**, *2*, 385–389; h) M. Cheng, X. Yang, S. Li, L. Sun, *Energy Environ. Sci.* **2012**, *5*, 6290–6293.

[3] a) Y. Bai, J. Zhang, D. Zhou, Y. Wang, M. Zhang, P. Wang, *J. Am. Chem. Soc.* **2011**, *133*, 11442–11445; b) S. M. Feldt, G. Wang, G. Boschloo, A. Hagfeldt, *J. Phys. Chem. C* **2011**, *115*, 21500–21507; c) S. M. Feldt, E. A. Gibson, E. Gabrielsson, L. Sun, G. Boschloo, A. Hagfeldt, *J. Am. Chem. Soc.* **2010**, *132*, 16714–16724; d) S. Cazzanti, S. Caramori, R. Argazzi, C. M. Elliott, C. A. Bignozzi, *J. Am. Chem. Soc.* **2006**, *128*, 9996–9997; e) H. Nusbaumer, J. E. Moser, S. M. Zakeeruddin, M. K. Nazeeruddin, M. Grätzel, *J. Phys. Chem. B* **2001**, *105*, 10461–10464; f) S. A. Sapp, C. M. Elliott, C. Contado, S. Caramori, C. A. Bignozzi, *J. Am. Chem. Soc.* **2002**, *124*, 11215–11222; g) K. B. Aribia, T. Moehl, S. M. Zakeeruddin, M. Graetzel, *Chem. Sci.* **2013**, *4*, 454–459; h) K. C. D. Robson, K. Hu, G. J. Meyer, C. P. Berlinguette, *J. Am. Chem. Soc.* **2013**, *135*, 1961–1971.

[4] A. Yella, H.-W. Lee, H. N. Tsao, C. Yi, A. K. Chandiran, M. K. Nazeeruddin, E. W.-G. Diau, C.-Y. Yeh, S. M. Zakeeruddin, M. Grätzel, *Science* **2011**, *334*, 629–634.

[5] a) R. M. Izatt, K. Pawlak, J. S. Bradshaw, R. L. Bruening, *Chem. Rev.* **1991**, *91*, 1721–2085; b) R. D. Hancock, A. E. Martell, *Chem. Rev.* **1989**, *89*, 1875–1914.

[6] a) H. I. Karunadasa, C. J. Chang, J. R. Long, *Nature* **2010**, *464*, 1329–1333; b) Y. Sun, J. P. Bigi, N. A. Piro, M. L. Tang, J. R. Long, C. J. Chang, *J. Am. Chem. Soc.* **2011**, *133*, 9212–9215; c) H. I. Karunadasa, E. Montalvo, Y. Sun, M. Majda, J. R. Long, C. J. Chang, *Science* **2012**, *335*, 698–702; d) M. Guttentag, A. Rodenberg, C. Bachmann, A. Senn, P. Hamm, R. Alberto, *Dalton Trans.* **2013**, *42*, 334–337.

[7] J. F. Endicott, G. Brubaker, T. Ramasami, K. Kumar, K. Dwarakanath, J. Cassel, D. Johnson, *Inorg. Chem.* **1983**, *22*, 3754–3762.

[8] R. A. Marcus, *Annu. Rev. Phys. Chem.* **1964**, *15*, 155–196.

[9] B. E. Hardin, H. J. Snaith, M. D. McGehee, *Nat. Photonics* **2012**, *6*, 162–169.

[10] M. K. Kashif, J. C. Axelson, N. W. Duffy, C. M. Forsyth, C. J. Chang, J. R. Long, L. Spiccia, U. Bach, *J. Am. Chem. Soc.* **2012**, *134*, 16646 – 16653.
[11] J. C. Yao, L.-F. Ma, F.-J. Yao, *Z. Kristallogr. New Cryst. Struct.* **2005**, *220*, 483 – 485.
[12] a) T. N. Mukarami, N, Koumura, T. Uchiyama, Y. Uemeura, K. Obuchi, N. Masaki, M. Kimura, S. Mori, *J. Mater. Chem. A* **2013**, *1*, 792 – 798; b) Z.-S. Wang, N. Koumura, Y. Cui, M. Takahashi, H. Sekiguchi, A. Mori, T. Kubo, A. Furube, K. Hara, *Chem. Mater.* **2008**, *20*, 3993 – 4003.
[13] a) A. Listorti, C. Creager, P. Sommeling, J. Kroon, E. Palomares, A. Fornelli, B. Breen, P. R. F. Barnes, J. R. Durrant, C. Law, B. O'Regan, *Energy Environ. Sci.* **2011**, *4*, 3494 – 3501; b) S. Guarnera, A. Bonucci, S. Perissinotto, R. Giannantonio, G. Lanzani, A. Petrozza, *RSC Adv.* **2013**, *3*, 2163 – 2166.
[14] a) C. Zhang, J. Dai, Z. Huo, X. Pan, L. Hu, F. Kong, Y. Huang, Y. Sui, X. Fang, K. Wang, S. Dai, *Electrochim. Acta* **2008**, *53*, 5503 – 5508; b) S. Nakade, Y. Makimoto, W. Kubo, T. Kitamura, Y. Wada, S. Yanagida, *J. Phys. Chem. B* **2005**, *109*, 3488 – 3493; c) F. Fabregat-Santiago, G. Garcia-Belmont, J. Bisquert, G. Boschloo, A. Hagfeldt, *Sol. Energy Mater. Sol. Cells* **2005**, *87*, 117 – 131; d) J. Krüger, R. Plass, L. Cevey, M. Piccirelli, M. Grätzel, U. Bach, *Appl. Phys. Lett.* **2001**, *79*, 2085 – 2087; e) S. Nakade, T. Kanzaki, W. Kubo, T. Kitamura, Y. Wada, S. Yanagida, *J. Phys. Chem. B* **2005**, *109*, 3480 – 3487; f) U. Bach, Y. Tachibana, J.-E. Moser, S. A. Haque, J. R. Durrant, M. Grätzel, D. R. Klug, *J. Am. Chem. Soc.* **1999**, *121*, 7445 – 7446; g) G. Boschloo, L. Haeggman, A. Hagfeldt, *J. Phys. Chem. B* **2006**, *110*, 13144 – 13150; h) S. Y. Huang, G. Schlichthorl, A. J. Nozik, M. Grätzel, A. J. Frank, *J. Phys. Chem. B* **1997**, *101*, 2576 – 2582; i) M. K. Nazeeruddin, A. Kay, E. Mueller, P. Liska, N. Vlachopoulos, M. Grätzel, *J. Am. Chem. Soc.* **1993**, *115*, 6382 – 6390.
[15] a) M. A. García-Monforte, S. Martínez-Salvador, B. Menjón, *Eur. J. Inorg. Chem.* **2012**, 4945 – 4966; b) M. Schlosser, M. Marull, *Eur. J. Inorg. Chem.* **2003**, 1569 – 1575; c) M. J. Katz, M. J. D. Vermeer, O. K. Farha, M. J. Pellin, J. T. Hupp, *Langmuir* **2013**, *29*, 806 – 814.
[16] T. Daeneke, A. J. Mozer, Y. Uemura, S. Makuta, M. Fekete, Y. Tachibana, N. Koumura, U. Bach, L. Spiccia, *J. Am. Chem. Soc.* **2012**, *134*, 16925 – 16928.

